ORGANOMETALLICS

Article

pubs.acs.org/Organometallics

Synthesis and Reactivity of Palladium Complexes Featuring a Diphosphinoborane Ligand

Tobias Schindler,[†] Marcel Lux,[†] Marius Peters,[†] Lennart T. Scharf,[†] Hassan Osseili,[†] Laurent Maron,[‡] and Michael E. Tauchert*[,†]

[†]Institute of Inorganic Chemistry, RWTH Aachen University, Landoltweg 1, 52056 Aachen, Germany

[‡]Université de Toulouse et CNRS INSA, UPS, CNRS, UMR 5215, LPCNO, 135 Avenue de Rangueil, 31077 Toulouse, France

Supporting Information

ABSTRACT: Synthetic access to the zerovalent palladium complexes {[(*o*-$Ph_2PC_6H_4)_2$BPh]Pd(L)} (L = pyridine (**8a**), 2,6-lutidine (**8b**)) is reported. Structural characterization and DFT analysis of **8a** revealed a strong Pd→B interaction, which appears to inhibit oxidative addition reactions. Activation of allyl acetate is possible by reversible transfer of the acetate leaving group to the ligand's borane functionality. Catalytic activity in the allylic substitution of allyl acetate with $HNEt_2$ is sensitive to the presence of free acetate, which reduces borane inhibition by reversible borate formation.

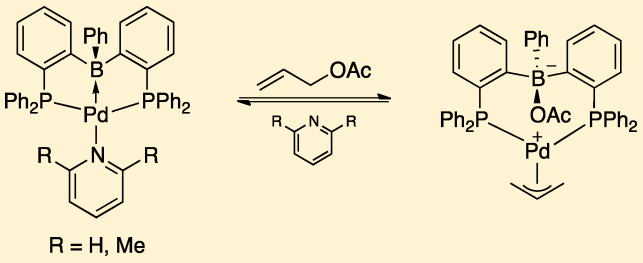

INTRODUCTION

Ambiphilic ligands, featuring L-type phosphorus or sulfur σ-donors as well as a Z-type σ-acceptor borane functionalities, possess unique coordination properties relevant to homogeneous catalysis.[1] Of particular note is their aptitude to form complexes with unusual high coordination numbers for a given oxidation state and their ability to withdraw electron density from the coordinated metal center by formation of a dative M→B bond.[1,2] These characteristics offer potential access to transition-metal catalysts with novel electronic and steric properties, unavailable with commonly employed L and X ligands. A Lewis acidic functionality of ambiphilic ligands can also interact directly with substrates.[3] Diphosphinoborane (DPB) ligands (*o*-$R^1{}_2PC_6H_4)_2BR^2$ (**1a−c**; Figure 1) are promising candidates to explore the potential of ambiphilic ligands for catalysis. Their structure and relatively large bite angle is similar to those of well-established chelating diphosphine ligands, such as DPEphos (bis[2-(diphenylphosphino)phenyl] ether). Recently, DPB ligands **1a−c** have been successfully applied in homogeneous catalysis such as transfer hydrogenation (Rh and Ir),[4a] hydrogenation (Ni[4b,c]), hydrosilylation (Ni),[4e] and enyne cyclization (Au).[4e] The Ru complex [((*o*-$Ph_2PC_6H_4)_2B(\eta^6$-Ph))RuCl][$B(C_6F_5)_4$] features an η^6-coordinated phenyl group, which is highly Lewis acidic and has been exploited in FLP-catalyzed aldimine hydrogenation.[4f,g] In addition to straightforward η^1-B coordination (**3**), ambiphilic ligands can adopt an η^2-B,C (**4**), or η^3-B,C,C (**5**) coordination mode.[4c,6,7] A "positive boryl effect" has also been reported for *o*-dimesitylphenylphosphine ligands $Mes_2B(o\text{-}R_2PC_6H_5)$. Pd-catalyzed Suzuki−Miyaura coupling reactions seem to profit from weak π-arene coordination of one mesitylborane group to the Pd center (**2**).[5] It has been suggested that strong M→B interactions might inhibit the coordinated metal's ability to perform oxidative addition reactions.[8] The coordination mode of the borane functionality appears to have a significant effect on the coordinated metal's reactivity toward substrates. While the Ni−(η^2-B,C) bond in complex **4** failed to react with H_2 at 60 °C, reversible activation of H_2 is readily observed at room temperature when employing complex **6**, in which ligand **1c** coordinates in an η^3-B,C,C coordination mode (Scheme 1).[4c] The example further demonstrates the ability of DPB ligands to interact with potential substrates. Despite its prevalence in numerous catalytic reactions, only two zerovalent Pd complexes

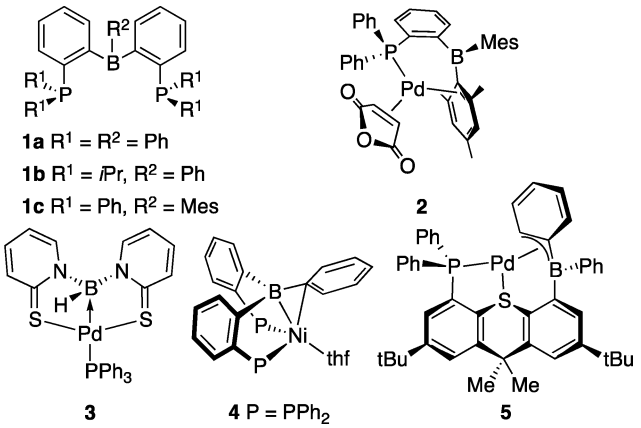

Figure 1. DPB ligands **1a−c** and selected complexes featuring different M→B coordination modes.[2a,b,4c,5a,6]

Received: March 17, 2015
Published: May 7, 2015

DOI: 10.1021/acs.organomet.5b00217
Organometallics 2015, 34, 1978−1984

Scheme 1. Reversible Activation of H_2[4c]

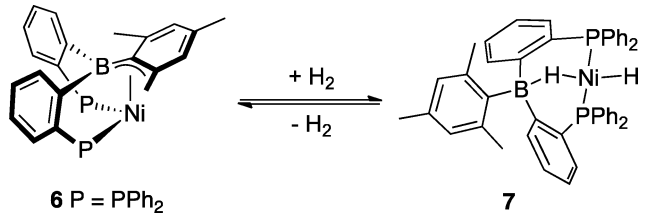

coordinated by chelating L_2Z ligands are known (**3** and **5**; Figure 1).[6] However, no catalytic applications have yet been reported for these complexes. In this paper we report the synthesis of Pd complexes featuring ambiphilic DPB ligands and explore their reactivity with regard to catalytic applications.

RESULTS AND DISCUSSION

Synthesis and Electronic Structure of Zerovalent Pd Complexes Featuring DPB Ligands. Synthesis of a zerovalent palladium complex was attempted by reaction of $(o\text{-}Ph_2PC_6H_4)_2BPh$ (**1a**) with 1 equiv of $CpPd(\eta^3\text{-}C_3H_5)$. Monitoring of the reaction by ^{31}P NMR spectroscopy indicated quantitative consumption of free ligand **1a** (δ −6.6) and formation of a new complex (δ 31.0). Meanwhile, ^1H NMR analysis revealed only 50% conversion of $CpPd(\eta^3\text{-}C_3H_5)$ toward its reductive elimination product 5-allylcyclopenta-1,3-diene (Scheme 2), indicating formation of the bisligand complex $\{[(o\text{-}Ph_2PC_6H_4)_2BPh]_2Pd\}$.

Scheme 2. Formation of Bisligand Complex

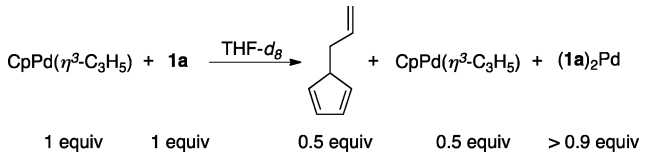

Reaction of $CpPd(\eta^3\text{-}C_3H_5)$ with the DPB ligand **1c** also produced a bisligand complex. In contrast, reaction of $(py)_2PdMe_2$ with ligand **1a** in THF-d_8 produced the complex $\{[(o\text{-}Ph_2PC_6H_4)_2BPh]Pd(py)\}$ (**8a**), featuring a single DPB ligand **1a** and one pyridine as a stabilizing coligand (Scheme 3)

Scheme 3. Synthesis of Zerovalent Pd Complexes 8a–c

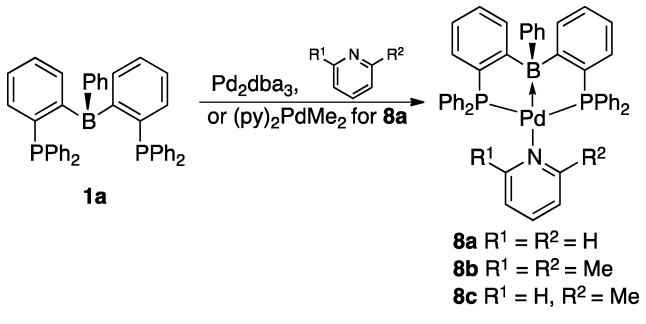

with 89% selectivity and 26% isolated yield. This complex **8a** is the first representative of the DPB ligand family coordinating to a zerovalent palladium fragment and, notably, also one of very few known examples of a zerovalent palladium complex featuring a monodentate nitrogen ligand.[9]

Pyridine complex **8a** showed a single resonance in the ^{31}P NMR spectrum at δ 31.0. The broad resonance observed in the ^{11}B NMR spectrum at δ 20 ($w_{1/2}$ = 400 ± 100 Hz) suggested a strong Pd→B interaction, on the basis of the proximity of the chemical shift to a tetravalent borate complex such as $NaBEt_4$ (δ −6) or $Et_3B{\cdot}NHMe_2$ (δ 4), rather than to the trigonal-planar free borane **1b** (δ 71 for **1b** in the ^{11}B solid-state NMR).[10]

Crystals of **8a** suitable for X-ray diffraction analysis were obtained by crystallization from benzene/hexane at room temperature (Figure 2). The coordination geometry around the

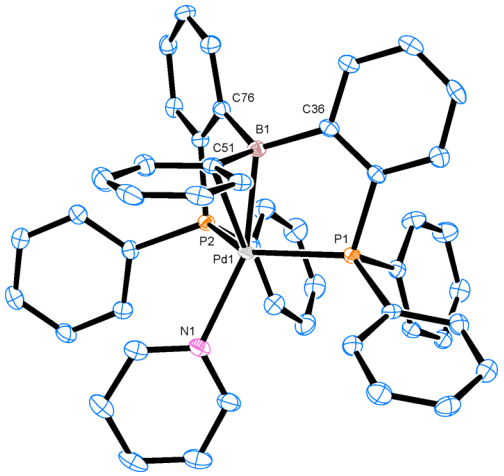

Figure 2. Thermal ellipsoid plots of **8a** depicted at the 50% probability level. Solvent and H atoms have been omitted for clarity.[11] Selected bond lengths (Å) and angles (deg): B1–C36 = 1.620(4), B1–C76 = 1.613(4), Pd1–N1 = 2.249(2), Pd–B1 = 2.194(3), Pd–C51 = 2.463(3), Pd–P1 = 2.2830(8), Pd–P2 = 2.2680(8), Pd–N1 = 2.249(2), B1–C51 = 1.610(4), N1–Pd1–P1 = 111.91(6), N1–Pd1–P2 = 100.33(6), N1–Pd1–B1 = 155.6(1), N1–Pd1–C51 = 117.02(9), B1–Pd1–P1 = 84.39(8), B1–Pd1–P2 = 82.99(8), P1–Pd1–P2 = 125.34(3).

palladium center is strongly distorted square planar, with the boron center located transoid to the pyridine ligand (N1–Pd1–B = 155.6(1)°). Significant pyramidalization is observed at the coordinating boron atom ($\sum B_\alpha$ = 346°). The complex features a short Pd–B distance (2.194(3) Å) and a short Pd–C51 distance (2.463(3) Å).[6] For all C–B bonds the same length of 1.61 Å is observed, suggesting a η^1-borane coordination mode, possibly augmented by an η^2-C,B interaction.[7] The Pd–N bond length of 2.249(2) Å is slightly elongated in comparison to the Pd–N bond in $[(py)_2Pd(ma)]$ (2.1472(19) Å; ma = maleic anhydride).[9a]

In order to gain additional insight into the bonding of the borane and pyridine ligands to the zerovalent palladium in **8a**, DFT calculations (B3PW91/Pd,P(SDD)/6-31G** (other atoms)) were carried out.[12] The optimized geometry of **8a** was found to be in excellent agreement with its solid-state structure. Bonds around the palladium center were especially well reproduced. The molecular orbitals were first analyzed. The HOMO-2 is a B–C to Pd interaction (Figure 3), whereas the HOMO-22 is a Pd–B bond. The bonding situation was investigated by NBO analysis. Similar Wiberg bond indexes were found for the Pd–B (0.478) and the Pd–P (0.549) interactions. In contrast, the Wiberg bond index for the C51–Pd interaction was found to be only 0.03, suggesting a donation from the B1–C51 bond rather than from the π density of the C51 atom only. At the second-order NBO level, a donation from an occupied d orbital of the palladium center to the empty p orbital of the boron ligand was found (113.0 kcal/mol) in line

DOI: 10.1021/acs.organomet.5b00217
Organometallics 2015, 34, 1978–1984

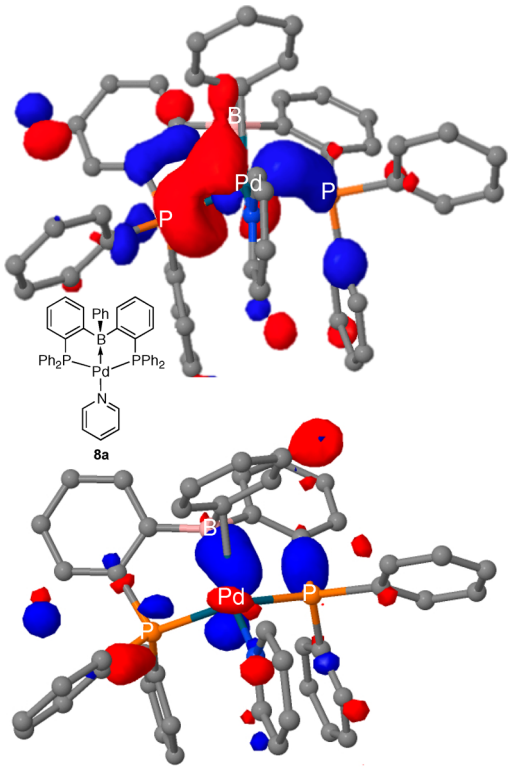

Figure 3. Molecular orbitals of complex **8a** (top) HOMO-2; (bottom) HOMO-22.

with a bonding interaction observed in the MOs. Additionally, a weaker donation from the C51–B1 bond to the metal center was observed (20 kcal/mol). Finally, the strength of the Pd–N(py) bond was analyzed. A dissociation enthalpy of 7.6 kcal/mol was observed for the Pd–pyridine interaction, with a Wiberg bond index of 0.256.

Next, we looked for a more convenient synthesis of **8a**, which would allow facile access to a broad range of coligands, avoiding the palladium precursor $(L)_2PdMe_2$. Reaction of DPB ligand **1a** with $Pd_2(dba)_3$ in the presence of 4 equiv of pyridine featured the desired Pd(0) complex **8a** in 60% isolated yield (Scheme 3). The same methodology was used to synthesize the 2,6-lutidine derivative **8b** as an analytically pure substance (54%). NMR analysis of **8b** revealed formation of a symmetric complex in the ^{31}P NMR spectrum (δ 30.4) as well as a strong Pd→B interaction comparable to that in **8a** (^{11}B NMR: δ 23, $w_{1/2}$ = 400 ± 100 Hz). Similarly, formation of the 2-picoline derivative **8c** was observed in an NMR experiment (^{31}P NMR: δ 33.7). The methodology could not be used to produce monoligated Pd complexes from DPB ligand **1c**.

Stoichiometric Reactivity. No reaction was observed at room temperature or 60 °C when an excess of phenyl bromide was added to complex **8a** or **8b**. The lack of reactivity could be caused by inhibition of the pyridine and/or the borane ligand. NMR experiments demonstrated that the pyridine ligand could be replaced by ligand metathesis. When 5 equiv of PPh_3 was added to a solution of **8b** in benzene-d_6, no exchange of the lutidine ligand was observed at room temperature or 50 °C. However, equimolar addition of PCy_3 resulted in fast and quantitative formation of the new complex {[(*o*-$Ph_2PC_6H_4)_2BPh$]Pd(PCy_3)}, featuring resonances at δ 22.8 and 32.5 in a 2:1 ratio in the ^{31}P NMR spectrum. A 3 equiv portion of PCy_3 led to the same result with significant broadening of the coordinated and free PCy_3 resonances, indicating a dynamic process between both species.

We therefore switched to an alkene substrate, which we expected to effectively be able to compete with pyridine/lutidine as a ligand. The reaction of complexes **8a**,**b** with 9 equiv of allyl acetate was monitored by ^{31}P NMR spectroscopy in benzene-d_6 (Scheme 4).

Scheme 4. Reversible Activation of Allyl Acetate

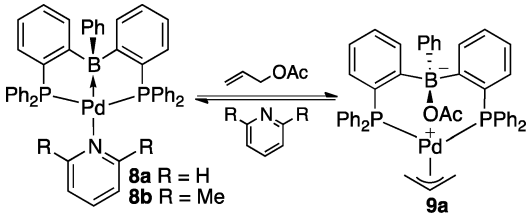

Reversible transformation into allyl complex **9a** was observed for both substrate complexes (^{31}P NMR δ 20.2). A slightly lower conversion of pyridine complex **8a** into allyl complex **9a** was seen after 48 h (68%), in comparison to that for lutidine complex **8b** (77%). This is in line with an expected lower binding constant of the lutidine ligand to the zerovalent palladium complex. Reaction of precursor **8b** with 27 equiv of allyl acetate allowed the isolation of allyl complex **9a** in 78% isolated yield by crystallization from benzene/hexane. Typical resonances for the allyl ligand were observed in the ^{13}C NMR spectrum (δ 73.1 and 116.4). ^{11}B NMR spectroscopy showed an upfield shift toward δ 3.3 ($w_{1/2}$ = 67 Hz), indicating the presence of a tetravalent borate. A similar oxidative addition process involving M→B bond cleavage and transfer of a leaving group has been observed: e.g., for the reaction of ferraboratrane $[(mim^{tBu})_3]Fe(CO)_2$ (mim^{tBu} = 2-mercapto-1-*tert*-butylimidazolyl) with $(PhC(O)O)_2$.[3c]

The solid-state structure of **9a** further confirmed coordination of the acetate to the boron center (Figure 4).

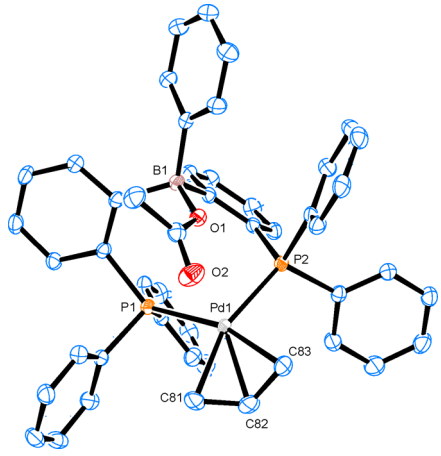

Figure 4. Thermal ellipsoid plots of **9a** depicted at the 50% probability level. Solvent and H atoms have been omitted for clarity.[13] Selected bond lengths (Å) and angles (deg) for **9a**: Pd1–P1 = 2.037(11), Pd1–P2 = 2.3922(7), Pd1–C83 = 2.148(2), Pd1–C82 = 2.162(2), Pd1–C81 = 2.197(3), O1–B1 = 1.527(3), B1–C51 = 1.651(3), P1–Pd1–Pd2 = 102.40(4), C82–Pd1–P1 = 123.69(7), C82–Pd1–P2 = 126.18(7).[14]

DOI: 10.1021/acs.organomet.5b00217
Organometallics 2015, 34, 1978–1984

The palladium center displayed a slightly distorted trigonal planar geometry with the two phosphine donors and the allyl ligand. Oxidative addition of allyl acetate to zerovalent palladium diphosphine complexes [(L-κ^2P)Pd^0] commonly results in the formation of cationic allyl complexes [(L-κ^2P)Pd^{II}(η^3-allyl)][OAc] with acetate as the counteranion (ligand = $(PPh_3)_2$, dppf, dppb).[14] In the DPB system the anticipated inhibiting effect of the strong Pd→B bond seems to be counteracted by simultaneous formation of the B−O bond in complex **9a**. Cleavage of the C−O bond of allyl acetate might be facilitated by intramolecular competition of the leaving group's lone pair with palladium for the ligand's Lewis acidic borane group, thus weakening the C−OAc bond as well as the inhibiting Pd→B interaction. Treatment of isolated allyl complex **9a** with pyridine or 2,6-lutidine in benzene-d_6 at room temperature resulted in the slow formation of zerovalent Pd complexes **8a,b**, respectively. The reaction progress was monitored by ^{1}H NMR and ^{31}P NMR spectroscopy at 50 °C for both pyridine (1 equiv) and 2,6-lutidine (2 equiv). The reaction reached >95% conversion within 35 h (see the Supporting Information, Figure S1). Within the margin of error identical reaction velocities were observed for formation of **8a,b**. Initial rate kinetics for the transformation of **9a** to **8b** were performed at 50 °C employing 2, 4, 8, and 16 equiv of 2,6-lutidine (see the Supporting Information, Figure S2). The reaction was found to be zero order in 2,6-lutidine. From these findings we conclude that reductive elimination is the rate-determining step of allyl acetate formation.

Using lutidine complex **8b**, we could observe C−O bond cleavage with allyl benzoate, producing complex **9b** (Table 1, entry 2). The conversion was considerably faster than that in the case of allyl acetate (Table 1, entry 1). Transfer of the leaving group to the ligand's Lewis acidic borane functionality was suggested by ^{11}B NMR spectroscopy. Formation of allyl borate complex **9c** was observed in the case of allyl trifluoroacetate, despite the low Lewis basicity of the trifluoroacetate leaving group and utilization of the coordinating solvent THF-d_8 (Table 1, entry 3). Allyl benzyl ether and allyl phenyl ether did not react at room temperature and were both heated for 17 h at 60 °C. Only allyl phenyl ether showed minor conversion (7%), but we were unable to verify whether an allyl complex had been formed.

Single crystals suitable for X-ray diffraction analysis could be grown from an NMR sample (benzene-d_6/hexane) of the allyl complex {[(*o*-$Ph_2PC_6H_4)_2$B(OBz)Ph]Pd(η^3-C_3H_5)} (**9b**; Figure 5), confirming transfer of the benzoate leaving group to the ligand's borane group. Reductive elimination of allyl benzoate from complex **9b** proceeded quickly, even in the absence of an N-heterocyclic coligand. When isolated crystals of **9b** were dissolved in THF-d_8 at room temperature a 1:1:1 mixture of **9b**, free allyl benzoate, and an unidentified Pd complex was observed within minutes.

Table 1. Reaction of Complex 8b with Allyl Substrates[a]

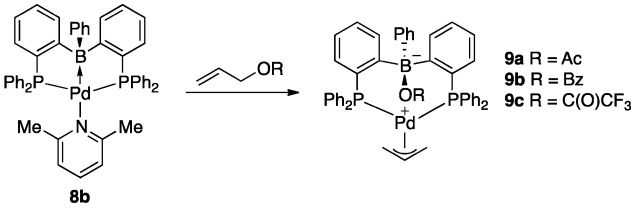

8b

#	Substrate	Conv. [%][b]	t [h]	^{31}P NMR [δ]	^{11}B NMR [δ]
1	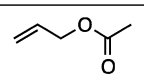	64[c]	20	20.2	3.3
2	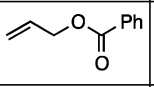	93	1	17.6	3.4
3	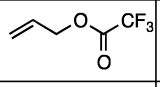	99	1	19.2[d]	4.5[d]
4	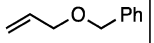	0[e]	17	-	-
5	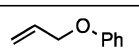	7[e]	17	18.0	n.d.

[a]Conditions unless noted otherwise: substrate:**8b** = 20:1, T = 23 °C, C_6D_6. [b]Monitored by ^{31}P NMR: [integral (product)]/[integral (all resonances)] × 100. [c]Allyl acetate:**8b** = 25:1. [d]Complex **8a**, allyl trifluoroacetate:**8a** = 4:1, THF-d_8. [e]T = 60 °C.

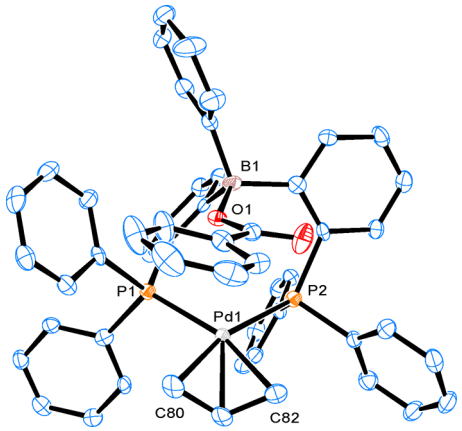

Figure 5. Thermal ellipsoid plots of **9b** depicted at the 50% probability level. Solvent and H atoms have been omitted for clarity. Selected bond lengths (Å) and angles (deg) for **9b**: Pd1−C80 = 2.163(5), Pd1−C81 = 2.168(5), Pd1−C82 = 2.207(5), Pd1−P1 = 2.3200(15), Pd1−P2 = 2.3965(14), O1−B1 = 1.552(7), P1−Pd1−P2 = 103.43(5).[15]

Catalysis. Complexes **8a,b** and **9a** were catalytically active in the allylic substitution reaction of allyl acetate with diethylamine featuring allyl amine **10** (Figure 6).[16]

The reactions were run as NMR experiments in benzene-d_6 at 60 °C, using 5 mol % of the respective catalyst and 1,2,3,4,5,6-hexamethylbenzene as internal standard. Due to the release of acetic acid during the reaction, 2 equiv of $HNEt_2$ was employed. Allyl complex **9a** displayed the highest activity in the reaction, followed by lutidine complex **8b** and pyridine complex **8a**. A plot of the concentration of the reaction product **10** versus time showed a concave curve when employing allyl complex **9a** as a catalyst. In contrast, sigmoid curves were observed for complexes **8a,b**. While acceleration of the reaction appeared not to be caused by removal of the potential inhibitor ligands pyridine and 2,6-lutidine by alkylation (monitoring by ^{1}H NMR spectroscopy) or protonation (excess of the more basic $HNEt_2$), the rates seemed to be affected by the accumulation of the acetate leaving group. Addition of 20 mol% of tetrabutylammonium acetate to a catalytic run employing **8a** as catalyst accelerated the reaction rate to a level similar to that monitored for allyl complex **9a**. Possibly,

DOI: 10.1021/acs.organomet.5b00217
Organometallics 2015, 34, 1978−1984

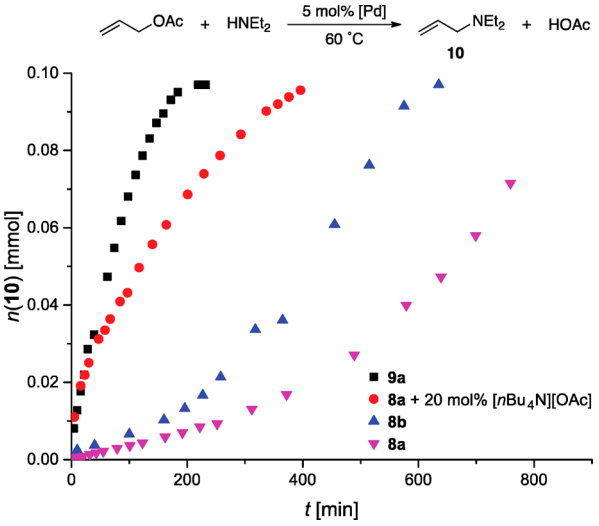

Figure 6. Monitoring (^{1}H NMR) of the allylic substitution of allyl acetate with $HNEt_2$ featuring **10**. Conditions: 194 μmol of $HNEt_2$, 97 μmol of allyl acetate, 24 μmol of C_6Me_6 (as internal ^{1}H NMR standard), 5 μmol of Pd complex, 0.75 mL of C_6D_6, T = 60 °C.

acetate competes with palladium for coordination to the Lewis acidic boron center, thus reducing—or eliminating—its aptitude to act as an inhibitor for the palladium catalyst. In this scenario the dominant catalytic species would be the acetate adduct complex $\{[(o\text{-}Ph_2PC_6H_4)_2B(OAc)Ph]Pd(L)\}^-$ formed in equilibration with $\{[(o\text{-}Ph_2PC_6H_4)_2BPh]Pd(L)\}$.

CONCLUSION

In conclusion, we prepared and characterized the first examples of zerovalent palladium complexes featuring a diphosphinoborane ligand $\{[(o\text{-}Ph_2PC_6H_4)_2BPh]Pd(L)\}$ (L = pyridine (**8a**), 2,6-lutidine (**8b**)). Complex **8a** displayed a strong η^1-B,Pd interaction in its solid-state structure, which was further examined by DFT methods. The ability of diphosphinoborane ligand **1a** to stabilize a zerovalent palladium fragment has important implications for future applications: (1) transformations involving a change of the oxidation state from Pd(II) to Pd(0) are likely to profit from such a stabilization, and (2) deposition of solid palladium particles during catalysis reducing catalyst longevity and/or leading to undesired side reactions should be reduced. The Pd→B interaction seemed to inhibit oxidative addition reactions toward the palladium center. Reversible C−O bond cleavage of allyl acetate and allyl benzoate, with transfer of the carboxylic leaving group to the ligand's borane function (allyl complexes **9a**,**b**), however, was feasible. A kinetic analysis of the allylic substitution reaction of allyl acetate with $HNEt_2$ was performed. Inhibition of the allylic substitution reaction by the Pd→B interaction was reduced in the presence of free acetate. We propose that inhibition by the borane functionality was reduced by partial reversible borate formation with acetate. Thus, interaction of the Lewis acidic site of ambiphilic ligands with Lewis bases plays an important role in catalysis, which will be the subject of further studies.

EXPERIMENTAL SECTION

All manipulations were carried out in an MBraun glovebox under an inert argon atmosphere. All glassware was dried in an oven at 120 °C overnight prior to use. NMR experiments were performed in Wilmad quick pressure valve NMR tubes. $^{11}B\{^1H\}$ NMR spectra were recorded in Norell natural quartz NMR tubes. ^{1}H, ^{11}B, ^{13}C, and ^{31}P NMR spectra were recorded on a Bruker Avance II (400.1 MHz, probe BBO) or a Bruker Avance (400.3 MHz, probe ATM BBFO) spectrometer. ^{1}H NMR spectra were referenced to residual solvent resonances (benzene-d_6, δ 7.16; THF-d_8, δ 1.72). $[(o\text{-}PPh_2C_6H_4)_2BPh]$ (**1a**)[8] and $[CpPd(\eta^3\text{-}C_3H_5)]$[17] were prepared according to the literature. Pyridine, 2,6-lutidine, and allyl acetate (all Alfa Aesar), benzene-d_6 and THF-d_8 (both Eurisotop), and diethylamine (Merck, 99%) were degassed employing the freeze−pump−thaw technique and dried over activated molecular sieves (4 Å). Tetrahydrofuran and pentane were dried by an MBraun solvent purification system. Benzene and *n*-hexane were dried over sodium and distilled under argon prior to use. $Pd_2(dba)_3$ was purchased from Sigma-Aldrich (97%) and used as received.

Synthesis of $\{[(o\text{-}PPh_2C_6H_4)_2BPh]Pd(pyridine)\}$ (8a). A 5 mL glass vial was charged with DPB ligand **1a** (0.100 g, 0.164 mmol, 1 equiv), pyridine (56.6 mg, 0.655 mmol, 4 equiv), and $Pd_2(dba)_3$ (75.0 mg, 0.082 mmol, 0.5 equiv). Benzene (3 mL) was added, and the suspension was stirred for 10 min at ambient temperature. The mixture was then filtered through glass wool and collected in a glass vial (5 mL) which was placed into a 20 mL glass vial containing *n*-hexane (ca. 5 mL). Within 3 days orange crystals precipitated from the benzene solution. The mother liquor was decanted, and the solid was washed with *n*-pentane and dried in vacuo (79 mg, 0.099 mmol, 60%). Crystals suitable for X-ray diffraction were taken from the crystal crop prior to drying in vacuo. Mp: 152 °C dec. ^{1}H NMR (400.1 MHz, benzene-d_6): δ 6.44 (ddd, J = 7.5, 4.3, 1.5 Hz, 2H), 6.80 (tt, J = 7.2, 2.1 Hz, 1H), 6.85 (m, 4H), 6.95 (m, 3H), 6.99 (m, 1H), 7.02 (m, 6H), 7.11 (m, 3H), 7.26−7.32 (m, 6H), 7.42−7.54 (m, 8H), 8.12 (dt, J = 4.1, 1.8 Hz, 2H), 8.26 (d, J = 7.8 Hz, 2H). $^{11}B\{^1H\}$ NMR (128.4 MHz, benzene-d_6): δ 20 ($w_{1/2}$ = 400 ± 100 Hz). $^{13}C\{^1H\}$ NMR (100.6 MHz, benzene-d_6): δ 123.7 (s), 126.0 (s), 125.7 (t, J = 2.9 Hz), 126.9 (s), 129.0 (s), 129.5 (s), 132.4 (s), 132.7 (s), 132.8 (s), 133.0 (t, J = 7.9 Hz), 133.8 (t, J = 7.8 Hz), 135.2 (s), 135.9 (t, J = 2.2 Hz), 137.9 (t, J = 14.7 Hz), 139.1 (s), 139.3 (s), 139.5 (t, J = 14.7 Hz), 151.1 (s). $^{31}P\{^1H\}$ NMR (161.9 MHz, benzene-d_6): δ 31.0. IR (KBr): $\tilde{\nu}$/cm^{-1} 3045, (w), 2997 (w), 2964 (w), 2926 (vw), 2853 (vw), 2262−2166 (w), 2080 (w), 1955 (vw), 1880 (vw), 1813 (vw), 1586 (w), 1478 (w), 1433 (m, sh), 1261 (w), 1155 (w, sh), 1092 (m, sh), 1066 (w), 1026 (m, sh), 860 (w), 802 (w, sh), 741 (s, sh), 721 (w), 694 (vs, sh), 627 (w), 600 (w), 509 (s, sh). Anal. Calcd for $C_{47}H_{38}BNP_2Pd$: C, 70.92; H, 4.81; N, 1.76. Found: C, 70.93; H, 4.94; N, 1.63.

Synthesis of $\{[(o\text{-}PPh_2C_6H_4)_2BPh]Pd(2,6\text{-lutidine})\}$ (8b). A 5 mL glass vial was charged with DPB ligand **1a** (0.200 g, 0.328 mmol, 1 equiv), 2,6-lutidine (144.5 mg, 1.310 mmol, 4 equiv), and $Pd_2(dba)_3$ (150.0 mg, 0.1640 mmol, 0.5 equiv). Benzene (3 mL) was added, and the suspension was stirred for 10 min at ambient temperature. The mixture was then filtered through glass wool and collected in a glass vial (5 mL) which was placed into a 20 mL glass vial containing *n*-hexane (ca. 5 mL). Within 3 days orange crystals precipitated from the benzene solution. The mother liquor was decanted, and the solid was washed with *n*-pentane and dried in vacuo (145 mg, 0.176 mmol, 54%). Mp: 168 °C dec. ^{1}H NMR (400.1 MHz, benzene-d_6): δ 2.25 (s, 6H), 6.48 (d, J = 7.0 Hz, 2H), 6.84 (td, J = 7.7 Hz, J = 0.9 Hz, 4H), 6.93 (t, J = 7.5 Hz, 3H), 6.98 (t, J = 7.5 Hz, 2H), 7.25 (m, 6H), 7.05 (m, 9H), 7.43 (m, 8H), 8.15 (d, J = 7.8 Hz, 2H). $^{11}B\{^1H\}$ NMR (128.4 MHz, benzene-d_6): δ 23 ($w_{1/2}$ = 400 ± 100 Hz). ^{13} C$\{^1H\}$ NMR (100.6 MHz, benzene-d_6): δ 24.6 (s), 119.9 (s), 126.0 (t, J = 2.6 Hz), 126.3 (s), 127.0 (s), 129.0 (s), 129.4 (s), 132.4 (s), 132.6 (s), 132.7 (s), 132.9 (t, J = 6.9 Hz), 133.6 (t, J = 7.8 Hz), 135.9 (s), 136.1 (s), 137.0 (t, J = 14.7 Hz), 138.3 (s), 138.4 (s), 138.5 (s), 138.6 (s), 138.8 (s), 158.2 (s). $^{31}P\{^1H\}$ NMR (161.9 MHz, benzene-d_6): δ 30.4. IR (KBr): $\tilde{\nu}$/cm^{-1} 3037 (w), 1599 (w), 1578 (w), 1477 (w), 1455 (m), 1431 (w), 1369 (w), 1265 (w), 1231 (w), 1182 (w), 1156 (w), 1123 (w), 1111 (w), 1091 (w) 1067 (w), 1026 (w), 998 (w), 852 (w), 774 (w), 761 (m), 742 (vs), 721 (m), 676 (m), 634 (w), 624 (m), 610 (w), 599 (m), 534 (w), 510 (s), 496 (m), 470 (w), 437 (w). Anal. Calc. for $C_{49}H_{42}BNP_2Pd$: C, 71.42; H, 5.14; N, 1.70. Found C, 71.69; H, 5.37; N, 1.63.

Synthesis of $\{[(o\text{-}PPh_2C_6H_4)_2B(OAc)Ph]Pd(\eta^3\text{-}C_3H_5)\}$ (9a). A 5 mL glass vial was charged with a solution of $\{[(o\text{-}PPh_2C_6H_4)_2BPh]$-

DOI: 10.1021/acs.organomet.5b00217
Organometallics 2015, 34, 1978−1984

Pd(lutidine)} (**8b**; 50 mg, 61 μmol, 1 equiv) in benzene (1.8 mL). Allyl acetate (165 mg, 1.65 mmol, 27 equiv) was added, and the mixture was stored overnight at ambient temperature. The vial was then placed in a 20 mL glass vial containing *n*-hexane, which was sealed. Within 40 h yellow crystals formed, which were isolated and washed with *n*-pentane (39 mg, 47 μmol, 78%). Mp: 128−138 °C dec. ^{1}H NMR (400.3 MHz, benzene-d_6): δ 1.64 (s, 3H, CH_3), 3.1−3.22 (m, 2H, H_{allyl}), 3.48−3.57 (m, 2H, H_{allyl}), 4.75−4.90 (m, 1H, H_{allyl}), 6.48−6.53 (m, 2H), 6.48−6.61 (m, 2H), 6.87−6.96 (m, 7H), 6.97−7.03 (m, 9H), 7.24−7.30 (m, 1H), 7.30−7.39 (m, 3H), 7.45−7.68 (br, 5H), 7.70−7.74 (m, 2H), 8.06−8.10 (m, 2H). ^{1}H NMR (400.3 MHz, THF-d_8): δ 1.24 (s, 3H, CH_3), 3.35- 3.45 (m, 4H, H_{allyl}), 5.57−5.69 (m, 1H, H_{allyl}), 6.26−6.34 (m, 2H), 6.46−6.53 (m, 2H), 6.88−6.94 (m, 1H), 6.95−7.01 (m, 5H), 7.03−7.12 (m, 5H), 7.12−7.22 (m, 11H), 7.40−7.48 (m, 5H), 7.54−7.57 (m, 2H). ^{11}B{^{1}H} NMR (128.4 MHz, benzene-d_6): δ 3.3 (s, $w_{1/2}$ = 67 Hz). ^{13}C{^{1}H} NMR (100.6 MHz, benzene-d_6) = δ 25.2 (s, OAc), 73.1 (s), 116.4 (s, C_{allyl}). ^{31}P NMR (162.0 MHz, benzene-d_6): δ 20.22 (s). ^{31} P{^{1}H} NMR (162.0 MHz, THF-d_8): δ 19.38 (s). IR (KBr): $\tilde{\nu}$/cm^{-1} 3090 (vw, sh), 3060 (w, sh), 3035 (m), 1957 (vw), 1813 (vw), 1690 (w, sh), 1652 (m), 1582 (w, sh), 1478 (m), 1447 (w), 1364 (m), 1288 (m), 1190 (w), 1182 (m), 1131 (m), 1093 (m), 1070 (w, sh), 1026 (m), 1001 (m), 938 (m), 851 (m), 821 (m), 728 (m), 746 (s), 696 (s), 678 (vs), 640 (m), 638 (m), 616 (m), 537 (m), 526 (m, sh), 510 (m, sh), 492 (m). Anal. Calc. for $C_{56}H_{50}BO_2P_2Pd$: C, 72.00; H, 5.39. Found C, 71.35; H, 5.24.

Synthesis of {[(*o*-$PPh_2C_6H_4)_2$B(OBz)Ph]Pd(η^3-C_3H_5)} (9b). Complex **8b** (22 mg, 0.026 mmol, 1 equiv) and allyl benzoate (15 mg, 0.094 mmol, 3.6 equiv) were weighed into a glass vial. Benzene (0.7 mL) was added, and the mixture was stirred for 10 min. The solution was then transferred into a Wilmad quick pressure valve NMR tube and immediately overlaid with hexane (0.4 mL). Within 24 h single crystals suitable for X-ray analysis were formed. ^{1}H NMR (400.1 MHz, THF-d_8): δ 2.23 (br s, 2H, CH_2), 3.40−3.30 (m, 2H, CH_2), 5.54−5.43 (m, 1H, *CH*). ^{11}B{^{1}H} NMR (128.4 MHz, THF-d_8): δ 4.5 ($w_{1/2}$ = 220 ± 50 Hz). ^{31}P{^{1}H} NMR (161.9 MHz, THF-d_8): δ 17.6 (s, $w_{1/2}$ = 180 Hz).

{[(*o*-$PPh_2C_6H_4)_2$B(O_2CCF_3)Ph]Pd(η^3-C_3H_5)} (9c; NMR Experiment). In a glovebox a glass vial was charged with complex **8b** (10 mg, 13 μmol, 1 equiv) and neat allyl trifluoroacetate (7.5 mg, 49 μmol, 4 equiv). THF-d_8 (0.7 mL) was added quickly, and the yellow solution was transferred to a Wilmad quick pressure NMR tube. NMR analysis was performed within 1 h. ^{1}H NMR (400.3 MHz, THF-d_8): δ 2.12 (bs, 2H, CH_2), 3.58 (bs, 2 H, CH_2), 5.54 (bs, 1H, *CH*). ^{11}B{^{1}H} NMR (128.4 MHz, THF-d_8): δ 4.5 ($w_{1/2}$ = 350 Hz). HSQC (400.3 MHz, THF-d_8): δ 2.12/75.08, 3.58/75.08, 5.54/118.00. ^{31}P{^{1}H} NMR (162.0 MHz, THF-d_8): 19.3 (s, $w_{1/2}$ = 11 Hz).

Reactivity Studies (Table 1, Entries 4 and 5). A stock solution of complex **8b** (20 mg, 7.0 μmol) in benzene-d_6 (1.00 mL) was prepared. The substrate (40 μmol, 20 equiv) was weighed into a 5 mL glas vial, and a stock solution of **8b** (0.3 mL, 2 μmol, 1 equiv) was added. The resulting solution was transferred by a Pasteur pipet to a quick pressure valve NMR tube. To secure quantitative transfer of the solution to the NMR tube, the glass vial was flushed with benzene-d_6 (2 × 0.2 mL), resulting in a total volume of 0.70 mL in the NMR tube.

Kinetics. A stock solution of $HNEt_2$ (57.8 mg, 0.790 mmol, 2 equiv), allyl acetate (40.1 mg, 40.1 μmol, 1 equiv), and hexamethylbenzene (15.3 mg, 94.3 μmol, 0.23 equiv) in benzene-d_6 (total volume 1.00 mL) was prepared. A 5 mL glass vial was then charged with the appropriate Pd complex (5.0 μmol), and 0.25 mL of the stock solution was added. The resulting solution was transferred with a Pasteur pipet to a quick pressure valve NMR tube. To secure quantitative transfer of the reagents to the NMR tube, the glass vial was flushed with benzene-d_6 (0.25 mL + 0.20 mL), resulting in a total volume of 0.70 mL in the NMR tube. The NMR tube was stored in an ice bath until commencement of the kinetic study. The reaction progress was monitored by ^{1}H NMR spectroscopy. In the case of complex **9a** the NMR tube was heated within the NMR machine to 60 °C. NMR tubes containing catalyst **8a** or **8b** were heated in a thermostated water bath (60.0 °C, Lauda ECO Silver thermostat). After the indicated heating period the NMR tubes were cooled in an ice bath for approximately 10 s. Complete cooling was demonstrated by solidification of benzene-d_6. ^{1}H NMR spectra were recorded after thawing of the sample.

■ ASSOCIATED CONTENT

Ⓢ Supporting Information

Text, figures, and CIF and XYZ files giving full experimental details, selected NMR spectra, Cartesian coordinates for optimized structure **8a**, and crystallographic data for CCDC 1049711 (**8a**), CCDC 1031952 (**9a**), and CCDC 1054024 (**9b**). The Supporting Information is available free of charge on the ACS Publications website at DOI: 10.1021/acs.organomet.5b00217.

■ AUTHOR INFORMATION

Corresponding Author

*E-mail for M.E.T.: Michael.Tauchert@ac.rwth-aachen.de.

Notes

The authors declare no competing financial interest.

■ ACKNOWLEDGMENTS

This work is dedicated to Prof. Dr. Peter Hofmann (University of Heidelberg) in recognition of his support and advice as "Doktorvater" of MET. We thank the Excellence Initiative of the German federal and state governments for financial support, the Chemical Industry Fund for a Liebig fellowship to M.E.T, the Hans-Böckler-Stiftung for a fellowship to T.S., and the Alexander von Humboldt Foundation for a fellowship to L.M. We are grateful to Dr. F. Pan and Dr. C. Merkens for collection of X-ray diffraction data and to Dr. T. P. Spaniol for help with structure refinement. The authors thank Prof. Dr. J. Okuda for generous support and helpful discussions and Prof. Dr. P. Hayes for valuable input.

■ REFERENCES

(1) (a) Kameo, H.; Nakazawa, H. *Chem. Asian J.* **2013**, *8*, 1720−1734. (b) Owen, G. R. *Chem. Soc. Rev.* **2012**, *41*, 3535−3546. (c) Emslie, D. J. H.; Cowie, B. E.; Oakley, S. R.; Huk, N. L.; Jenkins, H. A.; Harrington, L. E.; Britten, J. F. *Dalton Trans.* **2012**, *41*, 3523−3535. (d) Amgoune, A.; Bourissou, D. *Chem. Commun.* **2011**, *47*, 859−871. (e) Fontaine, F.-G.; Boudreau, J.; Thibault, M.-H. *Eur. J. Inorg. Chem.* **2008**, 5439−5454. (f) Braunschweig, H.; Dewhurst, R. D. *Dalton Trans.* **2011**, *40*, 549−558.

(2) (a) Bontemps, S.; Sircoglou, M.; Bouhadir, G.; Puschmann, H.; Howard, J. A. K.; Dyer, P. W.; Miqueu, K.; Bourissou, D. *Chem. - Eur. J.* **2008**, *14*, 731−740. (b) Sircoglou, M.; Bontemps, S.; Bouhadir, G.; Saffon, N.; Miqueu, K.; Gu, W.; Mercy, M.; Chen, C. H.; Foxman, B. M.; Maron, L.; Ozerov, O. V.; Bourissou, D. *J. Am. Chem. Soc.* **2008**, *130*, 16729−16738. (c) Sircoglou, M.; Bontemps, S.; Mercy, M.; Saffon, N.; Takahashi, M.; Bouhadir, G.; Maron, L.; Bourissou, D. *Angew. Chem., Int. Ed.* **2007**, *46*, 8583−8586.

(3) (a) Hazari, A.; Labinger, J. A.; Bercaw, J. E. *Angew. Chem., Int. Ed.* **2012**, *51*, 8268−8271. (b) Pang, K.; Tanski, J. M.; Parkin, G. *Chem. Commun.* **2008**, 1008−1010. (c) Figueroa, J. S.; Melnick, J. G.; Parkin, G. *Inorg. Chem.* **2006**, *45*, 7056−7058. (d) Kimmich, B. F.; Landis, C. R.; Powell, D. R. *Organometallics* **1996**, *15*, 4141−4146. (e) Börner, A.; Ward, J.; Kortus, K.; Kagan, H. B. *Tetrahedron: Asymmetry* **1993**, *4*, 2219−2228.

(4) (a) Kameo, H.; Nakazawa, H. *Organometallics* **2012**, *31*, 7476−7484. (b) Harman, W. H.; Lin, T. P.; Peters, J. C. *Angew. Chem., Int. Ed.* **2014**, *53*, 1081−1086. (c) Harman, W. H.; Peters, J. C. *J. Am. Chem. Soc.* **2012**, *134*, 5080−5082. (d) MacMillan, S. N.; Harman, W. H.; Peters, J. C. *Chem. Sci.* **2014**, *5*, 590−597. (e) Inagaki, F.; Matsumoto, C.; Okada, Y.; Maruyama, N.; Mukai, C. *Angew. Chem.,*

DOI: 10.1021/acs.organomet.5b00217
Organometallics 2015, 34, 1978−1984

Int. Ed. **2015**, *54*, 818−822. (f) Boone, M. P.; Stephan, D. W. *J. Am. Chem. Soc.* **2013**, *135*, 8508−8511. (g) Boone, M. P.; Stephan, D. W. *Chem. - Eur. J.* **2014**, *20*, 3333−3341.

(5) (a) Malacea, R.; Saffon, N.; Gómez, M.; Bourissou, D. *Chem. Commun.* **2011**, *47*, 8163−8165. (b) Malacea, R.; Chahdoura, F.; Devillard, M.; Saffon, N.; Gómez, M.; Bourissou, D. *Adv. Synth. Catal.* **2013**, *355*, 2274−2284.

(6) (a) Emslie, D. J. H.; Harrington, L. E.; Jenkins, H. A.; Robertson, C. M.; Britten, J. F. *Organometallics* **2008**, *27*, 5317−5325. (b) Zech, A.; Haddow, M. F.; Othman, H.; Owen, G. R. *Organometallics* **2012**, *31*, 6753−6760.

(7) For a recent review of η^2-B,C and η^3-B,C,C complexes see: Emslie, D. J.; Cowie, B. E.; Kolpin, K. B. *Dalton Trans.* **2012**, *41*, 1101−1117.

(8) Conifer, C. M.; Law, D. J.; Sunley, G. J.; White, A. J. P.; Britovsek, G. J. P. *Organometallics* **2011**, *30*, 4060−4066.

(9) (a) Kluwer, A. M.; Elsevier, C. J.; Bühl, M.; Lutz, M.; Spek, A. L. *Angew. Chem., Int. Ed.* **2003**, *42*, 3501−3504. (b) Canovese, L.; Visentin, F.; Chessa, G.; Uguagliati, P.; Dolmella, A. *J. Organomet. Chem.* **2000**, *601*, 1−15.

(10) (a) Nöth, H.; Vahrenkamp, H. *Chem. Ber.* **1966**, *99*, 1049−1067. (b) Landesman, H.; Williams, R. E. *J. Am. Chem. Soc.* **1961**, *83*, 2663−2666. (c) Bontemps, S.; Bouhadir, G.; Dyer, P. W.; Miqueu, K.; Bourissou, D. *Inorg. Chem.* **2007**, *46*, 5149−5151.

(11) Crystal data for **8a**: $C_{47}H_{38}BNP_2Pd$, M_r = 795.93, triclinic, space group $P\bar{1}$, T = 100(2) K, a = 10.010(2) Å, b = 10.217(2) Å, c = 20.291(5) Å, α = 86.589(4)°, β = 84.706(4)°, γ = 64.757(3)°, V = 1868.6(7) Å^3, Z = 2, μ = 0.618 mm^{-1}, 20935/10402 collected/unique reflections, R1 = 0.05, wR2 = 0.12, GOF = 1.073.

(12) This methodology has already been applied successfully to previous complexes featuring an M→B interaction. (a) Bontemps, S.; Gornitzka, H.; Bouhadir, G.; Miqueu, K.; Bourissou, D. *Angew. Chem., Int. Ed.* **2006**, *45*, 1611. (b) Sircoglou, M.; Bontemps, S.; Mercy, M.; Miqueu, K.; Ladeira, S.; Saffon, N.; Maron, L.; Bouhadir, G.; Bourissou, D. *Inorg. Chem.* **2010**, *49*, 3983−3990.

(13) Crystal data for **9a**: $C_{56}H_{50}BO_2P_2Pd$, M_r = 934.11, triclinic, space group $P\bar{1}$, T = 100(2) K, a = 9.874(2) Å, b = 14.424(3) Å, c = 18.105(4) Å, α = 66.69(3)°, β = 77.83(3)°, γ = 71.49(3)°, V = 2234.8(10) Å^3, μ = 0.530 mm^{-1}, Z = 2, 33952/12824 collected/unique reflections, R1 = 0.04, wR2 = 0.10, GOF = 1.055.

(14) Amatore, C.; Gamez, S.; Jutand, A. *Chem. - Eur. J.* **2001**, *7*, 1273−1280.

(15) Crystal data for **9b**: $C_{70}H_{61}BO_2P_2Pd$, M_r = 1113.34, orthorhombic, space group $Pna2_1$, T = 100(2) K, a = 19.511(4) Å, b = 15.966(3) Å, c = 17.786(4) Å, $\alpha = \beta = \gamma$ = 90°, V = 5541(2) Å^3, μ = 0.440 mm^{-1}, Z = 4, 58174/9841 collected/unique reflections, R1 = 0.04, wR2 = 0.11, GOF = 1.052.

(16) Complexes **8a,b** also catalyzed allylic substitution of allyl benzoate and cinnamyl 4-nitrobenzoate with $HNEt_2$.

(17) Tatsuno, O. S.; Yoshida, T.; Otsuka, S. *Inorg. Synth.* **1990**, *26*, 242−243.

DOI: 10.1021/acs.organomet.5b00217
Organometallics 2015, 34, 1978−1984